DETERMINING THE MOLECULAR MECHANISM OF TITIN-BASED LONGITUDINAL HYPERTROPHY IN SKELETAL MUSCLE

By

Yaeren Hernandez

A Thesis Submitted to the Faculty of the

DEPARTMENT OF CELLULAR AND MOLECULAR MEDICINE

In Partial Fulfillment of the Requirements

For the Degree of

MASTER OF SCIENCE

In the Graduate College

THE UNIVERSITY OF ARIZONA

2021

THE UNIVERSITY OF ARIZONA
GRADUATE COLLEGE

As members of the Master's Committee, we certify that we have read the thesis prepared by: Yaeren Hernandez
titled:

DETERMINING THE MOLECULAR MECHANISM OF TITIN-BASED LONGITUDINAL HYPERTROPHY IN SKELETAL MUSCLE

and recommend that it be accepted as fulfilling the thesis requirement for the Master's Degree.

Brett Colson
Brett Colson Date: Dec 13, 2021

John Konhilas Date: Dec 13, 2021

December 13, 2021

Final approval and acceptance of this thesis is contingent upon the candidate's submission of the final copies of the thesis to the Graduate College.

I hereby certify that I have read this thesis prepared under my direction and recommend that it be accepted as fulfilling the Master's requirement.

Brett Colson
Brett Colson Date: Dec 13, 2021
Committee Member
Cellular & Molecular Medicine

Acknowledgements:

The author would like to acknowledge her committee: Dr. Hendrikus Granzier, Dr. Brett Colson, Dr. John Konhilas, and Dr. Coen Ottenheijm for their guidance and help towards the development of this work.

She is grateful for the unconditional support and encouragement of her family: Carlos Estrada, Jose and Martha Hernandez. Her friends: Fernanda Garavito, Lauren Schulz, Tania Larrinaga, Chris Samper, Jason Giles, the Wilson-Badillo family, Holly Lopez and Barbara Kahn-Sales. Loved ones: Edwin Gonzalez, the McNeil Family, and Isele Jaramillo.

The author would also like to acknowledge members of the Granzier laboratory: Dr. Jochen Gohlke, Dr. Josh Strom, Dr. Robbert Van der Pijl, Dr. Marloes Van der Berg, Dr. John Smith, Justin Kolb, Zaynab Hourani, and Luann Wyly for their valuable input, technical support, and contributions to this work.

Table of Contents:

Table of Figures

Appendix

Abstract:

Longitudinal muscle hypertrophy is the lengthening of muscle fibers through the addition of sarcomeres in series. The molecular mechanisms of longitudinal hypertrophy are poorly understood. Identifying the factors that cause longitudinal hypertrophy is vital to developing therapeutic interventions to prevent muscle weakness in diseases such as cerebral palsy, chronic obstructive pulmonary disorder and fascioscapulahumeral muscle dystrophy. Titin, an ~4 MDa protein, spans from the Z-disk to the M-band of the sarcomere and maintains the structure of the sarcomere during stretch. Titin forms the molecular spring of the sarcomere and is ideally situated to sense mechanical signals. It has been proposed that titin regulates longitudinal hypertrophy by sensing muscle stretch and triggering mechano-sensitive signaling pathways that induce gene expression. I hypothesize that mechanically coupled vectors of titin regulate longitudinal hypertrophy in skeletal muscle, and therefore, an increase in titin-based stiffness will promote longitudinal hypertrophy. The $Ttn^{\Delta 112\text{-}158}$ mutant mouse model has a 47-exon deletion in the PEVK region of titin, the main spring region, which results in a stiffer titin molecule. By passively stretching muscles from WT and $Ttn^{\Delta 112\text{-}158}$ mice, the mechanisms by which titin promotes longitudinal hypertrophy was tested. This $Ttn^{\Delta 112\text{-}158}$ mouse model presented an ~34% increase in serial sarcomeres in skeletal muscle compared to control mice, making this an ideal model to study longitudinal hypertrophy. A series of *in vivo* and *ex vivo* experiments were performed, and proteomic techniques were used to identify changes in protein expression and post-translational modifications of skeletal muscle to uncover signaling proteins involved in longitudinal hypertrophy. The findings from these studies identified the PI3-AKT pathway involved in longitudinal hypertrophy. SPEG and synemin proteins were recognized as consistently being upregulated in $Ttn^{\Delta 112\text{-}158}$ stretched muscle compared to controls. These proteins associate with the Z-disk region and the M-Band region of titin, where phosphorylation activity is increased during muscle stretch. These studies further the understanding of muscle growth pathways and how skeletal muscle responds to mechanical signals providing insight into possible therapeutic targets for combating and treating muscle weakness in disease.

Introduction:

Skeletal muscles are organs that have many functions such as: voluntary movement, posture and balance maintenance, heat production, and protection of other vital organs in the body [1, 2]. Muscle forms during the embryogenesis stage; however, after birth muscles adapt to stimuli and environmental factors to become fully developed and functional [3]. Environmental stressors such as exercise, nutrition and loading conditions influence the function, size and shape of muscles [4]. Muscles are made from muscle fibers composed of sarcomeres. Sarcomeres are the basic functional contractile unit of muscle [5]. Sarcomere structure is highly conserved between all vertebrate animals and is similar to invertebrate animals with complex locomotion [3]

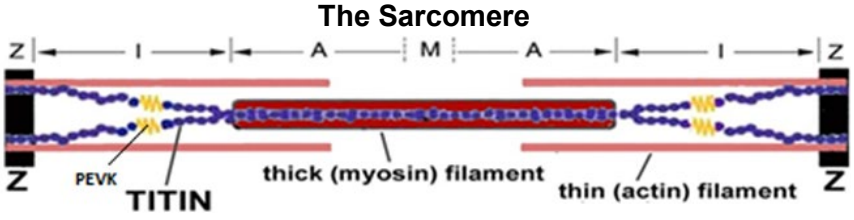

Figure 1: Illustration of the three filaments: titin (blue), thin filament (pink) and thick filament (red) within the sarcomere. Note the PEVK region (yellow) in titin, which contributes to its function as a molecular spring.
(Modified from: Ottenheijm C.A.C., Granzier H. (2010) Role of Titin in Skeletal Muscle Function and Disease. In: Muscle Biophysics. Advances in Experimental Medicine and Biology, vol 682)

Sarcomere

Skeletal muscle fibers are made up of sarcomeres, the basic contractile unit of muscle [5]. The boundaries of the sarcomere are from one Z-disk to another Z-disk with an M-line in the middle (Fig 1). The Z-disk contains proteins, such as alpha-actinin, desmin Cap-Z, that help anchor sarcomere filaments [3]. The M-Line contains proteins such as, myomesin and obscurin. Sarcomere filaments also anchor on the M-line. Within these stated boundaries there are three main filaments that make a sarcomere: 1) the thick filament, comprised primarily of myosin protein, attaches at the M-line; 2) the thin filament, which contains actin, attaches to the Z- disk; and 3) titin, the "molecular spring" of the sarcomere (Fig 1) which attaches from the Z-disk to the M-line. The proteins of the thick and thin filaments work together to generate active force during muscle contraction through cross-bridge cycling. Titin, the third filament, plays a role in maintaining sarcomere structure and generating passive force, protecting the sarcomere from damage when a muscle fiber is stretched [6]. These three filaments once assembled create highly regulated stable structures that do not spontaneously disassemble if it is isolated and stored properly [3].

Sarcomere Assembly

Proper sarcomeres formation is fundamental for muscle organization and function. Different genes regulate different production of sarcomeric proteins. During development proteins are synthesized in sequential order and undergo post translations modifications. Some proteins such as actin and myosin monomers spontaneously assemble intracellularly, however, they do not form sarcomeres on their own. Other proteins require an adenosine triphosphate (ATP) dependent chaperone, such as heat shock proteins (HsC70 and HsP90), for proper folding and positioning into sarcomere filaments, an example of this is the myosin heavy chain, the thick filament [7]. *In-vitro* cultured cell experiments demonstrated that mixtures of sarcomeric proteins (actin, alpha-actinin, myosin, titin etc) never assemble into sarcomere structures suggesting that temporal and spatial organization are important [3]. The following is a basic timeline of events for sarcomere assembly. First, muscle-specific intermediate filaments proteins: desmin, alpha-

actinin, and the Z-disk of titin are expressed and assemble onto an actin cytoskeleton filament [8, 9]. Then, the Z-disk of titin localizes with alpha-actinin and anchors alpha-actinin with actin leaving space for myosin insertion [10-12]. Second, sarcomeric-actin, sarcomeric myosin and M-band protein myomesin were produced as Z-disk titin begins unfolding exposing binding sites to assemble sarcomeres [13, 14]. Third, the M-band of the sarcomere begins to form. Titin-M-band epitopes coincide with the assembly of myomesin [13]. Myomesin connects myosin (thick filament) to the sarcomere, it maintains alignment of the thick filament and provides lateral elasticity. Fourth, myosin begins to integrate into the already assembled scaffold of the sarcomere; Z-disk, actin, titin, and M-Band [3, 13, 15]. Finally, other proteins such as: nebulin, myosin binding protein – C (MyBP-C), capping proteins etc integrate into the sarcomere to determine precise filament lengths, muscle function and maintenance [3, 16]. Formation of sarcomeres and muscle fibers in cultured cells have been insightful, the information that has been learned doesn't always translate well in *in-vivo* situations. For example: desmin is one of the first protein markers detected in skeletal muscle development, it is considered to be essential for sarcomere formation [17]. However, desmin knock-out mice were viable, and form sarcomeres but eventually developed problems with muscle maintenance and myopathies [18, 19]. Another example is with the protein titin; titin has been important for muscle fiber formations. It was observed that the complete removal of the titin gene does not allow for muscle fiber formation, even if the other sarcomeric proteins were expressed [20]. However, partial deletions of titin have been analyzed, some deletions (N2B mutation) lead to no formation of sarcomeres [21]; while other deletions in titin, Mex 1 and Mex2, does allow for sarcomere assembly [22].

Titin

Titin is the largest protein in the human body, ~4 MDa [23], and spans half the length of the sarcomere (>1μm) from the Z-disk to the M-line (Fig 1) [24]. The A-band region of titin stabilizes the thick filament, and the I-band region of titin is the "molecular spring." The molecular spring of titin is comprised of two spring elements, the tandem immunoglobulin (Ig) domains, and the PEVK (rich in proline, glutamate, valine, and lysine) region. Due to titin's size and position in the sarcomere, it is ideally situated to sense mechanical signals when the muscle tissue is stretched [25]. Titin, the molecular spring of the sarcomere, generates passive forces as the sarcomere stretches, preventing overstretch of sarcomere and muscle tissue [26, 27]. Titin helps keep the thick filament centered in the sarcomere, restores muscle length after release and prevents muscle damage, all of which are all critical for muscle contraction and mobility [28].

Passive Stiffness

Passive stiffness in muscle is defined as the resistance to elongation or shortening [29]. There are two components that contribute to muscle passive stiffness: the elastic component section and the viscous component [30]. The elastic component is not sensitive to velocity and is responsible for passive force generated when a muscle is held at a constant length reaching a steady-state of force. The elastic force elements were determined to be caused by entropic spring-like properties of titin (PEVK) and collagen [30, 31].

Unlike the elastic component, the viscous component is sensitive to velocity and is present only during stretching of the muscle. Viscous force elements are not as well understood; it is thought that multiple sources contribute to viscous force including the unfolding of Ig and fibronectin domains [30, 31]. The viscous force decays after repeated stretches at a constant length, known as stress relaxation [31]. Published work has shown that muscle phosphorylates several proteins: p38, JNK2, and p70s6k in response to repeated stretch [32]. These proteins have been associated with the transcriptional and translational control of protein synthesis [32]; however, their direct role in adding sarcomeres in series is not understood.

Hypertrophy:

Muscle hypertrophy is an increase of muscle mass by growth of muscle cells [33]. Many factors affect increase of muscle mass such as: muscle metabolism, mechanical tension, muscle damage, genetic factors, and hormones [34]. When muscle fails to respond to signals that lead to muscle hypertrophy, diseases such as muscle dystrophy, sarcopenia, weakness and decrease in range of motion and movement can occur. There are two types of muscle hypertrophy: concentric hypertrophy (cross-sectional growth) refers to the thickening of a cell, and eccentric hypertrophy (longitudinal growth) refers to the lengthening of a cell.

Cross-Sectional Hypertrophy

Cross-sectional hypertrophy is an increase in the diameter of a muscle cell resulting in thicker muscle tissue. Cross-sectional hypertrophy has been thoroughly studied and is associated with strength training and exercise and is triggered by repeated contractions when a muscle is under load (e.g., resistance training, lifting weights) [35, 36]. Many growth factors such as myostatin [37], insulin growth factor 1 [38], and calcineurin [39] have been documented to contribute to cross-sectional muscle growth.

Longitudinal Hypertrophy

Longitudinal hypertrophy occurs by increasing the number of sarcomeres in series resulting in muscle fiber lengthening. This type of hypertrophy occurs when skeletal muscle responds to an increase of strain by adding sarcomeres in series to lower the strain and maintain optimal sarcomere length. Longitudinal hypertrophy occurs as skeletal muscle develops and adapts to bone growth; once an organism has reached full maturation, fiber lengthening signals become dormant, although they can be triggered by surgical lengthening [40]. When skeletal muscle fails to stretch, muscle function such as movement and force production becomes compromised. Unlike cross-sectional growth, there is a gap in knowledge in the molecular mechanisms that drive longitudinal growth. During development, muscle experiences both types of hypertrophies, and this causes difficulties in identifying factors unique to longitudinal hypertrophy

Titin's Role in Hypertrophy and Protein Signaling Pathways

Titin has many functional regions where other proteins can bind: the Z-band, the center of the I-band region (spring region), and the M-line region (Fig 2) [41]. At present day, there are more than 20 binding proteins that link titin to diverse signaling pathways [42]. Some of titin's binding proteins are triggered through exercise, stretch, and eccentric contractions. Through these activities, the binding proteins activate signalling pathways that can travel between the cytoplasm and the nucleus leading to muscle hypertrophy [42]. The precise mechanical and molecular mechanisms driving longitudinal muscle hypertrophy have not been clearly understood or identified. An increase in longitudinal and cross-sectional muscle hypertrophy was discovered in a mouse model with a deletion in the C-terminus of the PEVK region ($Ttn^{\Delta 219-225}$) of titin [43], revealing that titin affects cross-sectional and longitudinal growth [43]. This study probed two protein synthesis pathways, the mTOR and Erk pathways to gain insight into the implicated hypertrophy signals; however, the signaling pathways were not conclusively resolved in this research [43]. Researchers propose that titin is a mechanosensory protein, regulating titin mechanically coupled vectors in response to stretch [44], and thereby causes changes in gene expression that result in longitudinal hypertrophy. Titin-binding proteins such as MLP [45, 46], MARP1-3[47-49], and MuRF1/2[50-52] have been implicated in muscle trophicity (Fig 2); however, titin's exact role in regulating the activation of these proteins is unclear.

Z-Band: Titin's Role in Hypertrophy and Protein Signaling Pathways

One example of a proposed mechanical stretch sensor leading to protein signaling is a complex formed with muscle LIMP-protein (MLP) located within the Z-disk (Fig 2) [45]. MLP contains a nuclear translocation signal that allows MLP to shuttle between the cytoplasm and the nucleus.

When MLP, T-Cap, and titin are activated, they have a direct link to hypertrophic signaling by interacting with the calcineurin/NFAT cascade, which results in translocation of NFAT to the nucleus triggering activation of genes [46]. As mentioned previously, calcineurin is a growth factor that has been identified in the involvement of cross-sectional hypertrophy. Perhaps there are other protein complexes within the Z-disk that are sensitive to stretch that could be linked to longitudinal growth pathways. Regardless, Z-disk proteins (alpha actinin, desmin, Z-disk of titin) are one of the first proteins expressed and assembled in the creation of new sarcomeres [3, 12, 53]. $Ttn^{\Delta 112\text{-}158}$ mouse model used in this project has more sarcomeres in series than WT [27] causing the Z-disk region to be oh high interest for longitudinal hypertrophy.

I-Band: Titin's Role in Hypertrophy and Protein Signaling Pathways

Muscle-ankyrin-repeat proteins (MARPs) have been shown to interact with the N2A region of the I-band [47] in titin (Fig 2). There are three MARP proteins: cardiac ankyrin repeat protein (CARP), diabetes related ankyrin repeat protein (DARP), and ankyrin-repeat-domain protein-2 (Ankrd2). MARPs have diverse functions within striated muscle. They play vital roles as transcriptional regulators in myofibrillar assembly [42]. There have been studies where all three MARPs are "knocked out" in skeletal muscle, which resulted in a more compliant muscle fiber with longer sarcomere lengths [48]. These MARPs knock-out muscle fibers expressed longer titin isoforms than wild type (WT) muscle fibers, indicating that MARPs interacting with titin may play a role in passive mechanical behavior of muscle [48]. The $Ttn^{\Delta 112\text{-}158}$ mouse model used in this project has a large section of the I-band deleted, theoretically affecting transcription regulation of MARP proteins in muscle fiber assembly, and protein interactions with titin

M-Band: Titin's Role in Hypertrophy and Protein Signaling Pathways

Another region for titin-mediated hypertrophic signaling is the M-band region, especially in the titin kinase domain (TK) of the M-band (Fig 2). When the TK domain is activated, it interacts with ubiquitin-associated zinc-finger protein neighbor of-BRCA1-gene-1 (Nbr1), which forms a signaling complex with p62/SQSTM1 and the muscle ring finger proteins MuRF1, MuRF2, and MuRF3 [53]. When MuRF1 and 2 are knock down, skeletal muscle undergoes hypertrophy suggesting that MuRF complexes inhibits hypertrophy signaling [42]. The TK domain is theorized to be activated by external forces such as mechanical stretch [25, 54], $Ttn^{\Delta 112\text{-}158}$ mouse model has a stiffer titin molecule perhaps affecting the TK domain, increasing its activation when stretched.

Disruptions in Titin-Binding Regions and Titin-Stiffness

Alterations in titin-binding regions or in titin-based stiffness, disrupts titin's role as a mechanosensor and affect protein pathways responsible for muscle growth. In diseases such as cerebral palsy (CP) and facioscapulohumeral muscle dystrophy (FSHD), muscle fibers with increased passive forces and alterations in titin stiffness have been demonstrated [55, 56]. Cerebral palsy patients have reported poor longitudinal growth by having increased sarcomere lengths, decrease sarcomeres in series, and changes in the extra-cellular matrix (ECM) [57]. The lack of longitudinal hypertrophy in CP patients leads to contractures which impair movement. Diaphragm fibers of patients with chronic obstructive pulmonary disorder (COPD) exhibit decreased passive stiffness due to a larger expandable titin region, which decreases muscle tension [58]. This causes the diaphragm to become flatten and limit its ability to contract and relax properly affecting respiration. These examples show how altered titin-based stiffness leads to disruption in muscle function. Further research in needed into titin's role as a mechanosensor affecting longitudinal hypertrophy.

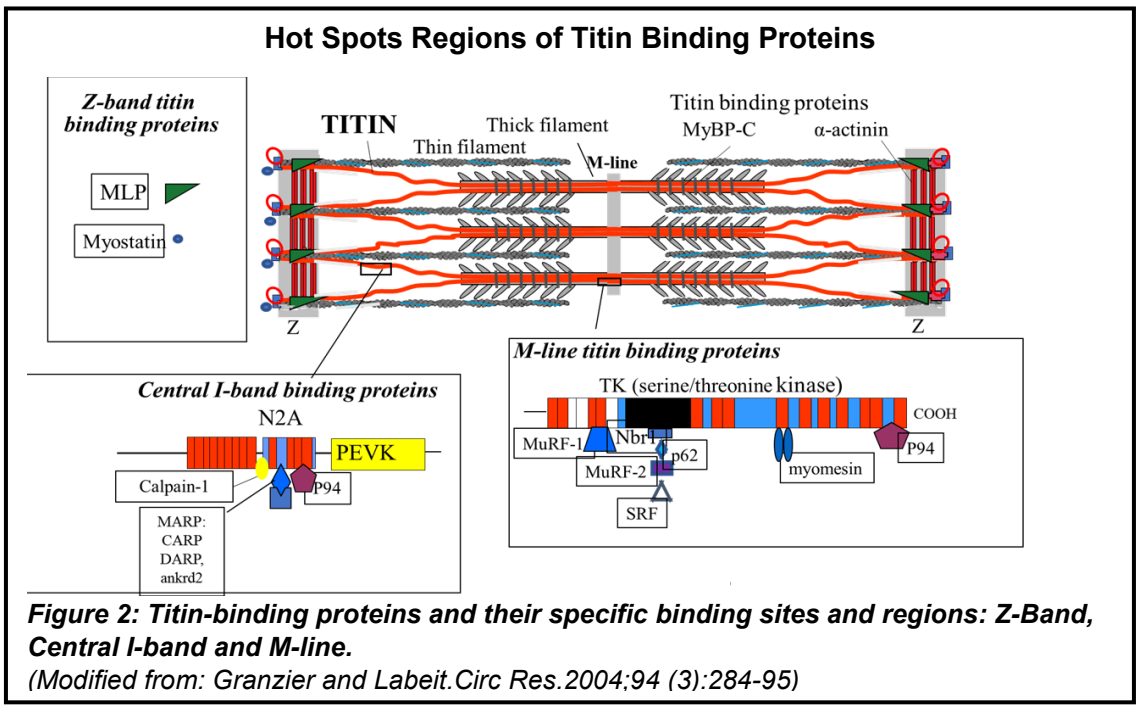

Figure 2: Titin-binding proteins and their specific binding sites and regions: Z-Band, Central I-band and M-line.
(Modified from: Granzier and Labeit.Circ Res.2004;94 (3):284-95)

Ttn$^{\Delta 112\text{-}158}$ Mouse Model

The Granzier lab developed the Ttn$^{\Delta 112\text{-}158}$ mouse model (Hom), to investigate the conflicting views of titin's contribution of passive stiffness generation on the whole muscle tissue [59]. The Ttn$^{\Delta 112\text{-}158}$ mouse model has a stiffer titin molecule due to the deletion of 47 PEVK exons that code for 1586 amino acids, resulting in a shorter titin spring region [27]. The exons deleted, exon 112 – 158, were not expressed in cardiac titin isoform [23]. The Ttn$^{\Delta 112\text{-}158}$ mouse model; therefore, is a skeletal muscle specific mutation. In comparison to WT mice, the Ttn$^{\Delta 112\text{-}158}$ mouse model showed an average 34% increase in sarcomeres in series in various skeletal muscles with no cross-sectional growth making this mouse model ideal to study titin's role in longitudinal hypertrophy [27].

Materials and Methods:

All experiments in this study were conducted to comply with the NIH guide for the Care and Use of Laboratory Animals [60]. All experiment and animal handling were approved by IACUC (University of Arizona's Institutional Animal Care and Use Committee) protocols (#09-095.)

Mice:

All Ttn$^{\Delta 112\text{-}158}$ mice used in this study were created and bred as described in Brynnell et al. [27]. The Ttn$^{\Delta 112\text{-}158}$ mutant mouse model has an increased titin-based stiffness used to identify titin's mechanosensing properties and evaluate the promotion of longitudinal hypertrophy. The Ttn$^{\Delta 112\text{-}158}$ mutant mouse model has a 47-exon deletion in the PEVK region, the main spring region of titin, which results in a stiffer titin molecule. All mice were born in Mendelian ratios and there was no difference in skeletal growth between the genotypes. Interestingly, this mouse model presented an ~34% increase in serial sarcomeres in skeletal muscle, making this mouse model useful to study longitudinal hypertrophy.

5th Toe EDL Muscle Mechanics:

The protocol used for muscle mechanics, was a passive stretch protocol from Hornberger et al. with minor modifications [32], such as the method of flash freezing muscle and using cell culture solution to better suit the purpose of the project. This protocol has proven that repeated stretch phosphorylates several proteins that are associated with transcriptional and translational control of protein synthesis [32]. This protocol can cause detectable changes to the proteome and affect protein synthesis. Two-month-old mice were anesthetized with isoflurane and then sacrificed with a cervical dislocation. The 5th toe extensor digitorum longus (EDL) muscle from both legs were quickly dissected from tendon to tendon, the muscle was weighed, and then metal rings made of insect pins were sutured on to both distal and proximal tendons of the muscle. The muscles were placed in a heated 37 °C chamber filled with a 95/5 O_2/CO_2 oxygenated high glucose Dulbecco's Modified Eagle Medium (DMEM) solution (Gibco) containing: 4.5 g/L D-glucouse, L-glutamate and no sodium pyruvate additive. The stretched 5th toe EDL was attached to a distal end high speed length controller (Aurora Scientific Models 322C-I) on one end and a force transducer (Aurora Scientific Models 402A) on the other end, and then placed in a chamber with the DMEM media. Sarcomere lengths of the 5th toe EDL were measured through laser diffraction (class 3B Milles Griot 25-LHR-991-249 laser). The muscle was stretched at a 50 ms ramp from slack length to a sarcomere length of 2.8 μm; then held at this length for 100 ms. Afterwards, it was quickly released (50 ms) back to its original length. This stretch-and-release motion was repeated every 3 seconds for 90 total minutes, totaling 1800 stretches. Control unstretched muscle was treated identically to the stretched muscle but held at a static slack length for 90 min.

The passive stretched forces produced by the 5th toe EDL were normalized by calculating the physiological cross-sectional area (PCSA) of the muscle, taking into account its unique unipennate architecture. Unipennate muscles have fibers that are oriented at one fiber angle to the force generating axis and are all on the same side of a tendon [61, 62]

The PSCA of the 5th toe EDL was calculated by using the following equation:

$$\text{PCSA } (\text{cm}^2) = \frac{\text{muscle mass (g)} * \cos(\theta)}{\rho(g\ cm^{-3}) * fiber\ length\ (cm) * fiber\ ratio} \quad [63]$$

θ was the pennation angle calculated at 11.3% and ρ is the physiological density of muscle at 1.056kg/L = 1056mg/ml and a fiber ratio of 69% for the 5th toe [62]. After experiments, muscles were quickly submerged in liquid nitrogen and saved for proteomic analysis. There are four experimental groups that were analyzed: stretched WT and $Ttn^{\Delta 112\text{-}158}$ muscle, and unstretched WT and $Ttn^{\Delta 112\text{-}158}$ muscle. Each group has 30mg of tissue, averaging eight to twelve mice since the 5th toe EDL weighs and average of 3-4 mg

Hind Limb Cast:

The protocol used for the hindlimb cast experiment is a modified protocol from Dayanidhi, S., et al. [64]. At four months of age, mice were anesthetized with isoflurane while their right hindlimb was immobilized in a plantar flexion position by placing a Velcro-cast for two weeks. This immobilization forced the shortening of the soleus muscle and the lengthening of the EDL muscle. Mice kept their hindlimb immobilized for two weeks, until the cast was removed. Two time points of data were taken: the first time point was the day the cast is removed, and the second time point was 3.5 days after the cast is removed. The contralateral leg was not casted and served as a control. Mice were anesthetized with isoflurane and then sacrificed with a cervical dislocation. The leg muscles of soleus, plantaris, gastrocnemius, tibialis cranialis (TC) and extensor digitorum longus (EDL) from both casted leg and the uncasted leg were dissected and weighed.

The soleus muscle was pinned on a cork board past slack length and fixed in a 4%

paraformaldehyde solution. The rest of the muscle tissue was flash frozen and saved for further analysis. This process was repeated at the second time point after 3.5-day recovery. Mice that had their Velcro-cast removed were allowed to recover through normal movement for 3.5 days

Measuring Sarcomeres in Series:

Fixed soleus muscle tissue length was measured with calipers and high-magnification optical microscopy. Fibers were dissected from tendon end to tendon end and the length was measured. Fiber tissue was placed on a microscope slide and sarcomere lengths were measured with laser diffraction (class 3B Milles Griot 25-LHR-991-249). Ten sarcomere measurements were made across the whole fiber, and eight muscle fibers were dissected per sample. The average of all the measurements was reported. With these measurements, sarcomeres in series were calculated by multiplying the fiber length by the sarcomere lengths.

Muscle Solubilization for Mass Spectrometry:

The protocol for muscle solubilization has been previously described [65] with minor modifications. Those modifications were that muscle samples were solubilized in 8M Urea Buffer at 10x sample weight and bromophenol blue was not included in the 8M Urea Buffer. Muscles were grouped together by their experimental group, to reach an ideal group weight of ≥30 mg.

Mass Spectrometry:

Muscle samples analyzed through mass spectrometry were sent to the state-of-the-art Proteomics Core at the University of Arizona, using bioanalytical expertise and instrumentation to perform matrix-assisted laser desorption/ionization (MALDI) mass spectrometry (MS). The MALDI-MS technique determined protein quantification, phosphorylation, and other post-translational changes. A gel base fractionation method was used for a better resolution of the whole muscle proteome. The gel base fractionation method separates proteins by their size (important for densely populated muscle tissue, containing many proteins of various sizes). The gel was the cut into various sections and were processed through MS for a better resolution of the whole proteome. Enrichment of phosphorylation protocols was also performed, where 4-5 mg of muscle lysate was used to perform one experimental run on the MS instrument. Typically, 40-50 mg of muscle tissues will generate 4-5 mg of lysate. Since mouse muscles have low tissue weights, muscle tissue of various mice was pooled into an experimental group to achieve the required lysate mass requirement. In pilot experiments, we determined that 30 mg of tissue generating 3 mg of lysate was sufficient to obtain reliable phosphorylation enrichment results. The lysate sample was processed through an affinity binding column to separate out phosphorylated proteins and then ran through MS. As individual mouse leg muscles have low weights, muscle tissues (5^{th} Toe EDL) of various mice, were pooled in each experimental group to achieve the lysate mass required for high quality data with suitable signal to noise.

Protein Analysis

Mass spectrometry experiments detected and extracted a list of peptides known as Uniprot ID's. A mapping table was used for UniprotKB identifiers and Ensembl gene ID's were added to each peptide using R to enable downstream analysis [66]. Individual modifications were determined for each peptide and modifications, other than phosphorylation, were removed from the dataset. Positions of modified residues were determined to be located in the exact positions of phosphorylation within the protein sequence. Protein sequences were downloaded with Uniprot.ws using UniprotKB identifiers [67]. Phosphorylated positions were located using pattern matching with stringr [68].

In heat map generation, the rows were scaled by subtracting the mean and dividing by standard deviation. Peptides were hierarchically clustered with hclust [65] and heat map were visualized with pheatmap [69]. In order to determine differentially enriched peptides, abundance values

were vsn-normalized and missing data was imputed using random draws from a manually defined left-shifted gaussian distribution (shift=1.8, scale=0.3) [70]. Analysis of variance (ANOVA) with Tukey's honest significant test (HSD) was used to determine significantly differential peptides between all groups in the heat maps. Analysis of significant changes was done with Limma for selected comparisons [71]. A protein's sample variance was shrunk towards a pooled estimated increased reliability and power of detecting significant changes. Differences in peptide abundance were visualized on regular volcano plots with EnhancedVolcano[7] [72] and on interactive volcano using Plotly [73].

For Kyoto Encyclopedia of Genes and Genome (KEGG) analysis, the most significantly changed peptide per gene were filtered out and differential pathways were determined based on perturbation of the pathway and over-representation analysis with ROntoTools[9] [74]. Pathways of interest were visualized with Pathview [75].

Statistical Analysis

Some statistical analysis was done using GraphPad Prism Software 9. Comparisons between the two genotypes were done using one or two-way ANOVA analyses to establish differences. A t-test was used to find differences between different groups. All values are shown as mean and ± standard deviation; p-value < 0.05 was considered significant. The labels were showed as p-value ≤ 0.05 is "*", p-value ≤ 0.01 is "**" and p ≤ 0.005 is "***".

Results

5th Toe EDL Muscle Mechanics:

The 5th toe EDL was chosen for this experiment for three main reasons. 1) The EDL is a muscle that has proven to experience longitudinal hypertrophy in Ttn$^{\Delta 112\text{-}158}$ mouse model [27]. 2) The 5th toe EDL muscle can be dissected from tendon-to-tendon end without injury to muscle fibers, making it useful for intact mechanics. 3) The 5th toe EDL is a thin muscle that allows for sarcomeres in series to be measured by laser diffraction. Previous literature established that whole muscle tissue from Ttn$^{\Delta 112\text{-}158}$ mice has higher passive tension when stretched in comparison to the WT mice [27], and the results using the 5th toe EDL were consistent with previous research (Fig 3). Figure 3 shows the passive force normalized to the physical cross-sectional area of the 5th Toe EDL. Ttn$^{\Delta 112\text{-}158}$ muscle has higher passive tension than WT, when the muscle is stretched to a sarcomere length of 2.8 µm and quickly released. The graph also shows a decay in force in both WT and Ttn$^{\Delta 112\text{-}158}$ mice as the number of stretches increases. This was expected and is known as stress-relaxation [31]. Ttn$^{\Delta 112\text{-}158}$ mice exhibits has a greater decay in force than WT mice because experiences greater strain than WT

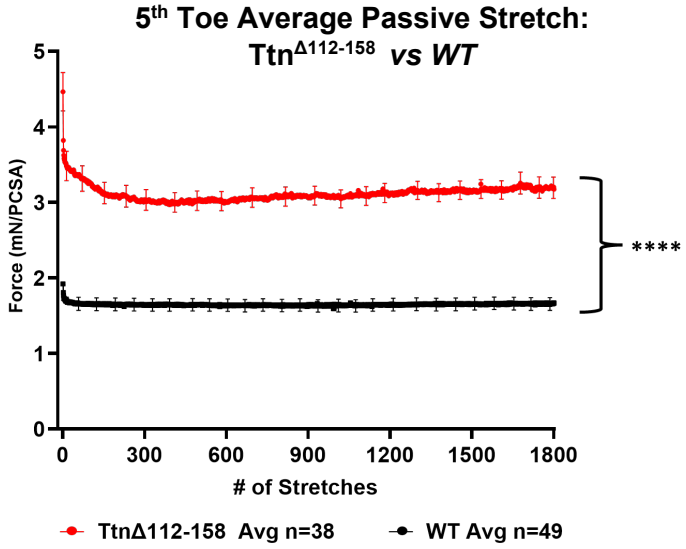

Figure 3: Average 5th toe passive stretch: **Ttn$^{\Delta 112\text{-}158}$** ***vs WT with standard error of mean; **** indicates p-value < 0.0001. Ttn$^{\Delta 112\text{-}158}$ mice (n=38) labeled by red circle. WT mice (n=49) labeled by black circle***

mice due to a shortened titin molecule

During the collection of samples, it was observed that the stretched tissue has an increased weight after the experiment that is more pronounced in $Ttn^{\Delta 112\text{-}158}$ stretched muscle group compared to the WT stretched muscle group in both sexes (Fig 4, left graph). The $Ttn^{\Delta 112\text{-}158}$ male stretched muscles have a significant weight increase ($p < 0.0001$) (Fig 4, left graph) after the experiment. This weight increase was not seen before the experiment in baseline conditions (Fig 4, right graph).

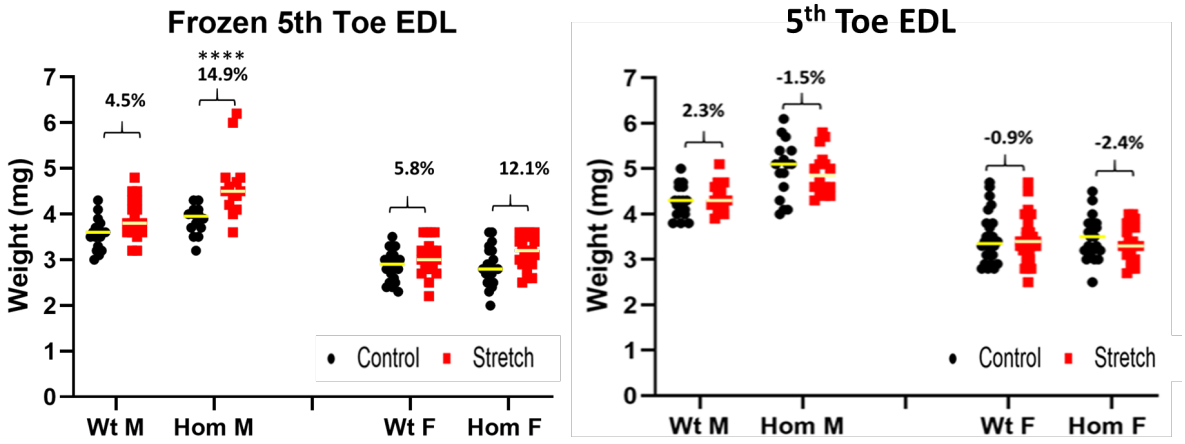

Figure 4: Raw tissue weights of 5th toe EDL muscle.
Left graph is of the weight of frozen 5th toe EDL of tissue of WT and $Ttn^{\Delta 112\text{-}158}$ ***after the experiment, seperated by genotype and sex. Black circle is the control muscle condition. Red square is the stretch muscle condition. WT male mice had a 4.5% increase in weight in the stretch condition compared to control.*** $Ttn^{\Delta 112\text{-}158}$ ***male mice had a 14.9% increase in weight in the stretch condition compared to control(**** p < 0.0001). WT female mice had a 5.8% increase in weight in the stretch condition compared to control.*** $Ttn^{\Delta 112\text{-}158}$ ***female mice had a 12.1% increase in weight in the stretch condition compared to control***
Right graph is the tissue wieghts of the 5th toe EDL of before the experiment, seperated by genotype and sex. Black circle is the control muscle condition. Red square is the stretch muscle condition. WT male mice had a 2.3% increase in weight in the stretch condition compared to control. $Ttn^{\Delta 112\text{-}158}$ ***male mice had a 1.5% decrease in weight in the stretch condition compared to control. WT female mice had a 0.9% decrease in weight in the stretch condition compared to control.*** $Ttn^{\Delta 112\text{-}158}$ ***female mice had a 2.4% decrease in weight in the stretch condition compared to control***

5th Toe EDL Muscle Proteomics:

There were four experimental groups per sex, stretched WT and $Ttn^{\Delta 112\text{-}158}$ muscle and unstretched WT and $Ttn^{\Delta 112\text{-}158}$ muscle. 30 mg of grouped muscle tissue was used for each group (n=2). Preliminary analysis of the mass spectrometry data on the 5th toe EDL experiment has provided insights into specific pathways and proteins associated with longitudinal growth. The heat map in Figure 5 showed 1,368 significant different phosphorylated peptides based on

normalized abundance values. The heat map is organized into clusters based on the behavior of the peptides, as opposed to function of the peptides *per se*. The heat map clusters showed differences based on sex, genotype, and treatment (Fig 5). Cluster one had the most peptides grouped together. In cluster one, male control $Ttn^{\Delta 112\text{-}158}$ groups had peptides in a higher abundance value compared to male stretched $Ttn^{\Delta 112\text{-}158}$ groups. Although the abundance value was different between male control $Ttn^{\Delta 112\text{-}158}$ groups and female control $Ttn^{\Delta 112\text{-}158}$ groups the trend was similar in which the proteins were elevated in $Ttn^{\Delta 112\text{-}158}$ control muscle versus $Ttn^{\Delta 112\text{-}158}$ stretch muscle. Cluster one showed a difference caused by treatment (Fig 5). Cluster six grouped higher abundance peptides based on sex. All male experimental groups had higher expression of peptides versus all female experimental groups. Cluster four peptides were grouped based on higher abundances in both control and stretched $Ttn^{\Delta 112\text{-}158}$ muscle compared to control and stretched WT muscle in both sexes. Cluster five illustrated grouped peptides that were higher in abundance in WT control and stretched muscles in both sexes (Fig 5). Both clusters four and five showed a difference based on genotype. Out of the 1,368 significantly different phosphorylated peptides in the heat map (Fig 5), 204 of them were phosphorylated titin peptides. Phosphorylated titin peptides accounted for 15% of the total significant peptides.

Figure 6 is a parallel coordinate that plot that displays values of phosphorylated titin peptides, using the same data as a heat map (Fig 5),as a different visual. The parallel coordinate plot displayed the results and behaviors of individual peptides across experiment. Figure 6 showed Titin PEVK 18 peptides, from cluster one, were down regulated in $Ttn^{\Delta 112\text{-}158}$ stretch and $Ttn^{\Delta 112\text{-}158}$ unstretched muscle groups. Titin PEVK 18 is deleted in the $Ttn^{\Delta 112\text{-}158}$ mice. This method of graphing helped to verify that there were no errors made when grouping muscles into the various experimental groups.

Figure 7 is a chart of the number of modifications per domain and location within titin. This chart compares all WT stretched muscle (blue) versus all $Ttn^{\Delta 112\text{-}158}$ stretched muscle (red). Although this data has not been normalized, an increased amount of phosphorylation in the titin kinase region (TK/M band region) and the Z-disk region of titin was revealed in $Ttn^{\Delta 112\text{-}158}$ mice. These regions of titin were investigated as hot spots involved in stretch response and pathway signaling. The PEVK region of titin has very little modifications this could be due to the fact that many exons from this region have been deleted, and therefore no phosphorylation is occurring in those sites.

Muscle Growth Pathways

Phosph-KEGG Pathway Analysis has elicited research into the PI3K-AKT signaling pathway. The PI3K-AKT signaling pathway is an intracellular signal transduction pathway that promotes metabolism, proliferation, cell survival, growth, and angiogenesis in response to extracellular signals [76]. This pathway is essential to postnatal muscle growth and hypertrophy. Phosphorylated proteins in the PI3K-AKT pathway appeared to be up or down regulated in $Ttn^{\Delta 112\text{-}158}$ stretched muscle compared to WT stretched muscle (Fig 8A). Fig 8B shows the affected proteins highlighted in the pathway with the LogFC value and p-value. Heat Shock Proteins, HSP90aa1, and HSP90ab2, are chaperone proteins that bind to other proteins during translation, and thereby stabilize them [77, 78]. These proteins have increased fold change differences alluding to higher protein translation occurring in $Ttn^{\Delta 112\text{-}158}$ stretched muscle. Mitogen-activated protein kinases, MAP2k2 and MAPK1, are extra cellular signaling regulated kinases that are involved in many cellular processes such as proliferation, differentiation, and regulation of transcription. These kinases play a role in mitogen growth factor signal transduction and activate the MAPK1/ERK2 and MAPK3/ERK1 pathways [79]. These proteins are all down regulated (Fig 8A and 8B). Figure 9 is a volcano plot, depicting the stretch differences among 22,712 peptides between WT and $Ttn^{\Delta 112\text{-}158}$, 12,114 of these peptides have a negative fold change and 10,598 have a positive fold change. Upon further investigation it was revealed that kinase suppressor of Ras 1 is elevated (Fig 9). Kinase suppressor of Ras 1 has an

increase in fold change that is significant, therefore blocking activity in the Ras-Raf-MEK-ERK pathway. This elevation in kinase expression could explain why MAP2k2 and MAPK1 are down regulated in the PI3K-AKT signaling pathway.

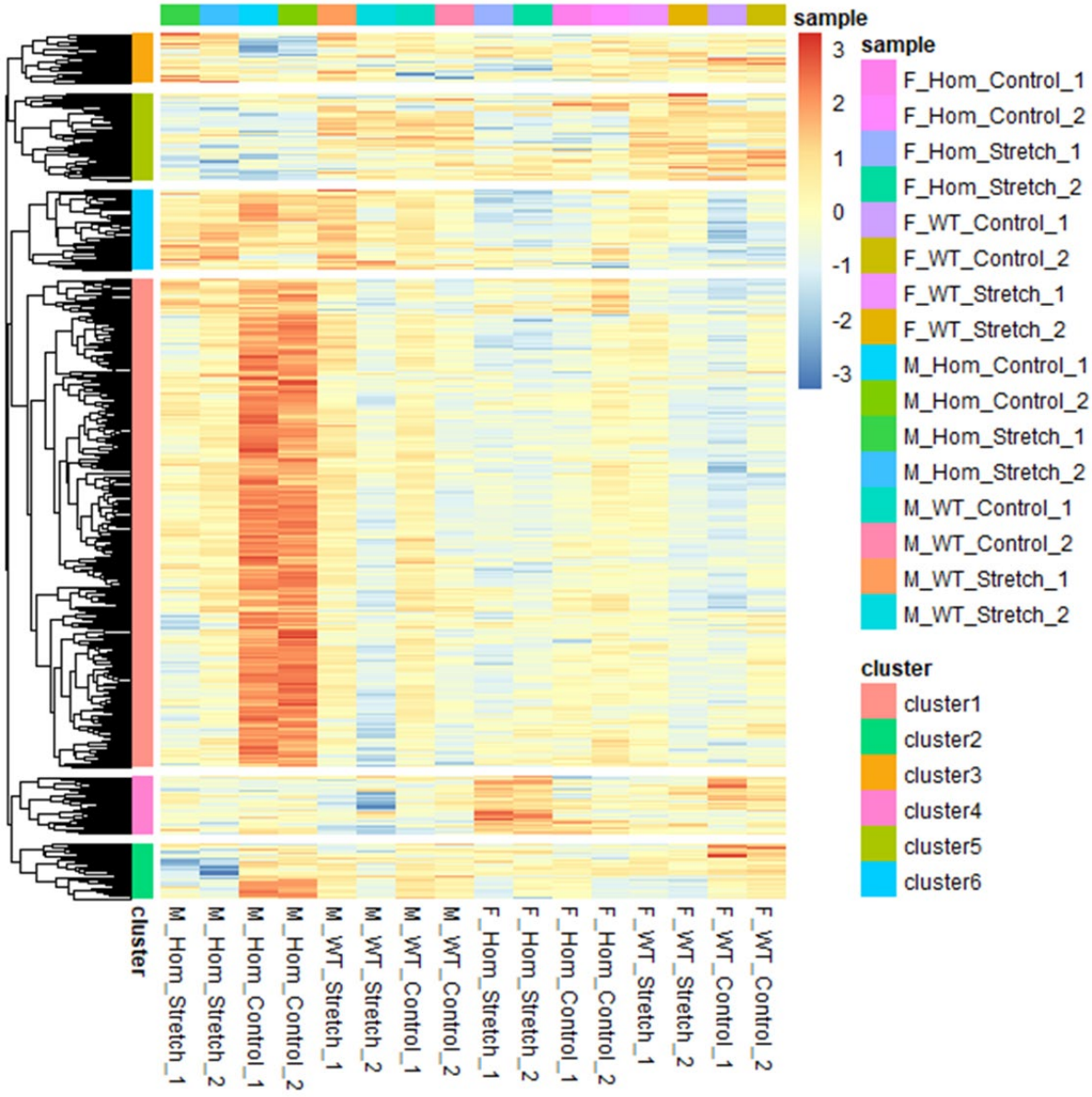

Figure 5: Heat map of the most significant phosphorylated peptides based on normalized abundance values. Phosphorylated peptides are clustered based on similarties of values. Clusters depict diffrence in phospho-peptides by sex, genotype and treatment.

Coordinate Plots: Phosphorylated Peptides Behavior

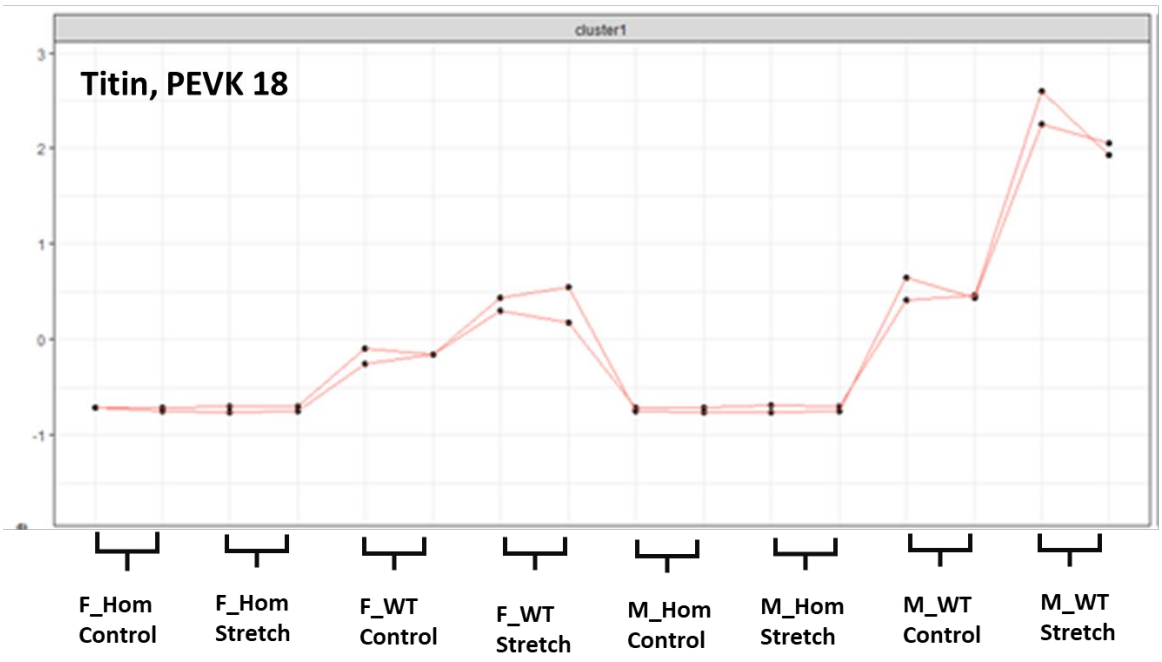

Figure 6: Parallel Coordinate plots of phosphorylated peptides: Titin phosphorylated peptide PEVK18 from Cluster 1 is down reglated in Female (F) and Male (M) $Ttn^{\Delta 112\text{-}158}$ (Hom). PEVK18 is a region of titin that is deleted in $Ttn^{\Delta 112\text{-}158}$ mutant mouse and present in wild type (WT).

Localization of differential titin phosphorylation

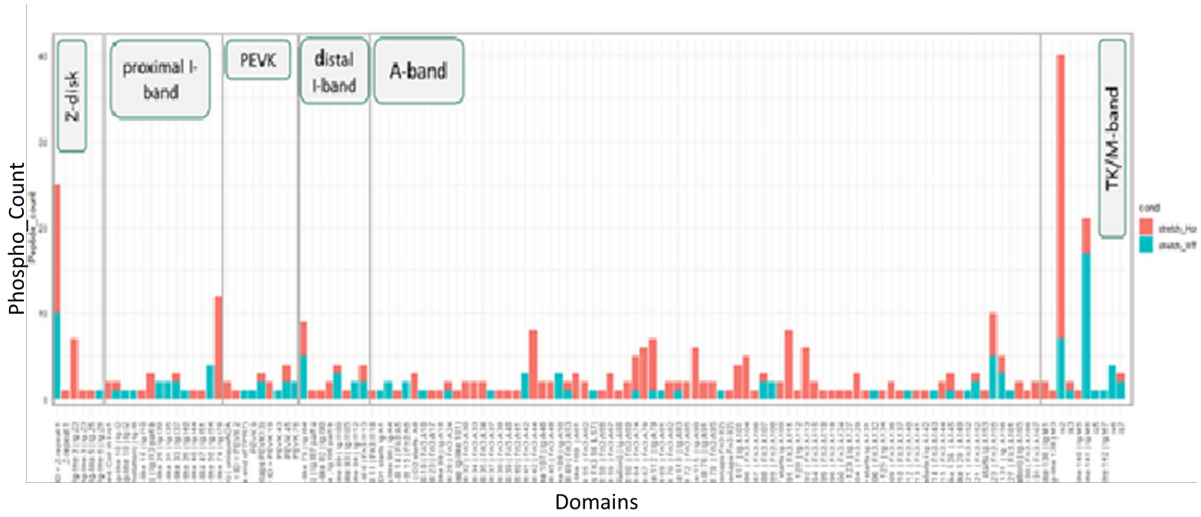

Figure 7: Chart of titin domain phosphorylation modifications, comparing all WT stretched muscle (blue) versus all $Ttn^{\Delta 112\text{-}158}$ stretched muscle (red). Many modifications were located in the TK/M-band region and the Z-disk region of titin.

Pathway Chart of PI3-AKT

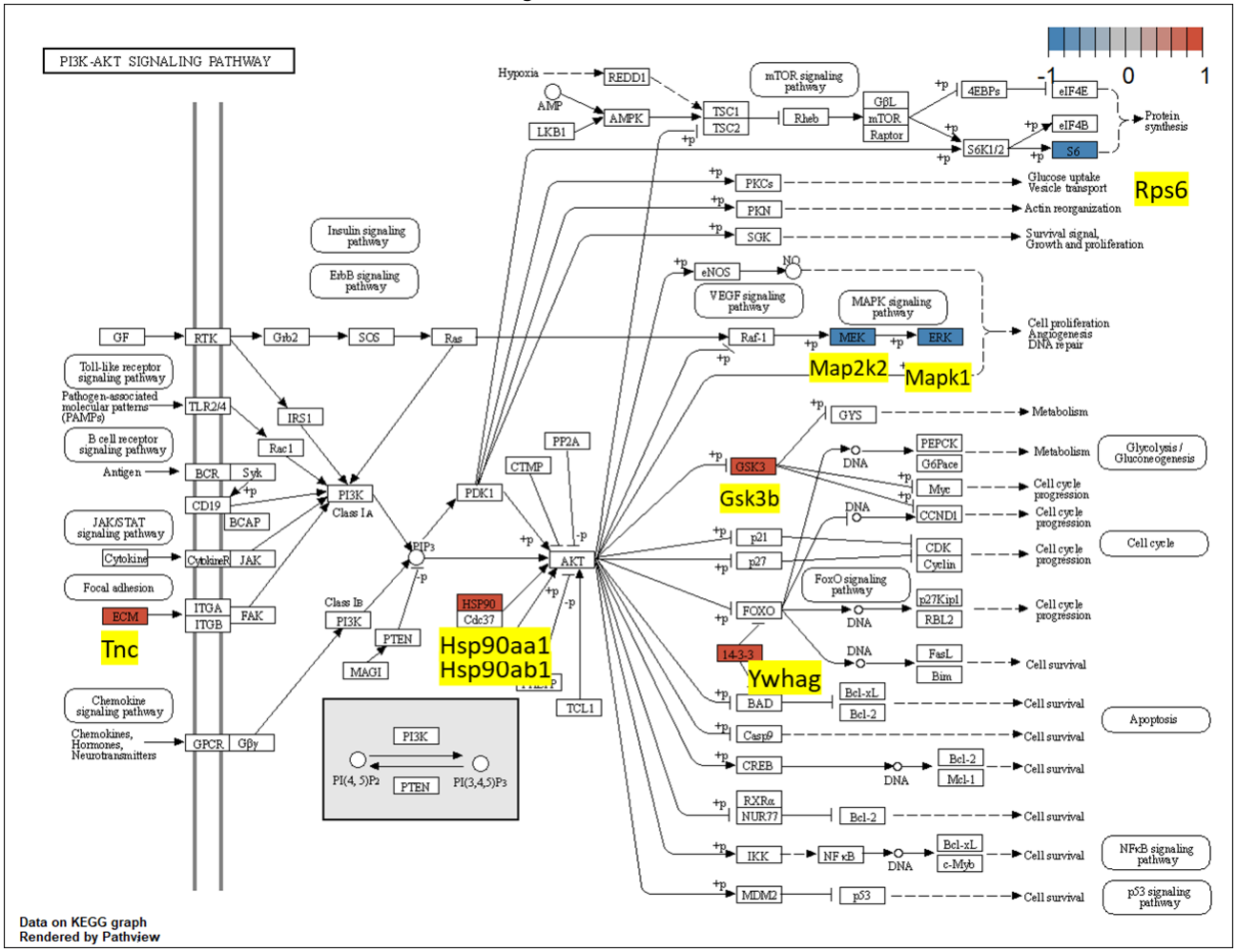

Figure 8A: PI3-AKT pathway with highlighted proteins that are significantlly up or down regulated based on the $Ttn^{\Delta 112\text{-}158}$ versus WT stretched muscle.

Highlighted Proteins

Uniprot	logFC_S.diff	P_S.diff
Hsp90ab1	75263048	0.070
Hsp90aa1	162473.6	0.118
Rps6	-1.9E+07	0.052
Tnc	131378.6	0.018
Ywhag	69039.1	0.186
Map2k2	-2278848	0.006
Mapk1	-96978.1	0.176
Gsk3b	430216.4	0.081

Figure 8B: Table of highlited proteins from PI3-AKT pathway with LogFC diffrence values and p-values

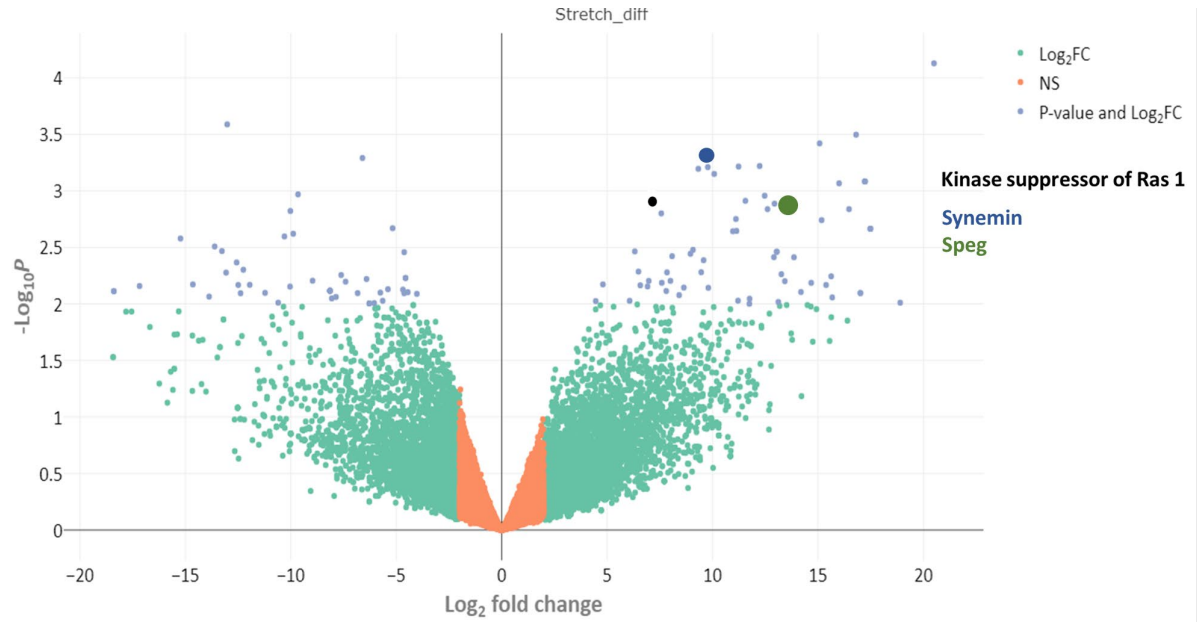

Figure 9: Volcano plot showing WT and* Ttn$^{\Delta 112\text{-}158}$ *stretched muscle peptides differences. Peptides are displayed by Log$_2$FC value (x-axis)and p-value (y-axis).

Hind Limb Cast:

To avoid confounding factors of normal growth in *in vivo* experiments. Mice at 4 months of age were chosen for this experiment because their rapid growth phase slows down between 2 -3 months of age and becomes steady after 4 months of age. After a 2-week immobilization casting experiment, sarcomeres in series from the soleus muscle of WT and Ttn$^{\Delta 112\text{-}158}$ mice were measured and analyzed (Fig 10). WT and Ttn$^{\Delta 112\text{-}158}$ non-recovered group were mice that once their cast was removed, their tissue was fixed for analysis. This shows the sarcomere absorption of ~8% between WT not recovered control muscle (2818, ± 261) and WT non-recovered casted muscle (2309 ± 212) being in a consistent range with previous studies [64, 80]. WT mice lost an average of 36 sarcomeres a day. Ttn$^{\Delta 112\text{-}158}$ non-recovered control muscle (3618 ± 265) compared to Ttn$^{\Delta 112\text{-}158}$ non-recovered casted muscle (2640 ± 120) had an ~27 % decrease averaging a loss of 70 sarcomeres a day. Ttn$^{\Delta 112\text{-}158}$ mice had a greater rate of sarcomere absorption than WT. The next time point measured was the WT and Ttn$^{\Delta 112\text{-}158}$ recovered casted group. Mice were allowed to move around for 3.5 days after their cast was removed. WT recovered casted muscle (2682 ± 465) had an ~12% increase from the WT non-recovered casted time point. Overall, in 3.5 days WT casted recovered group improved by an average of 104 sarcomeres per day. Ttn$^{\Delta 112\text{-}158}$ recovered casted muscle (2844 ± 188) had an ~8% improvement, increasing 80 sarcomeres per day. There was difference between the two time points of measurements of sarcomere in WT and Ttn$^{\Delta 112\text{-}158}$ (WT $p < 0.016$, and Ttn$^{\Delta 112\text{-}158}$ $p < 0.041$) ; however, there was no difference between the genotypes .

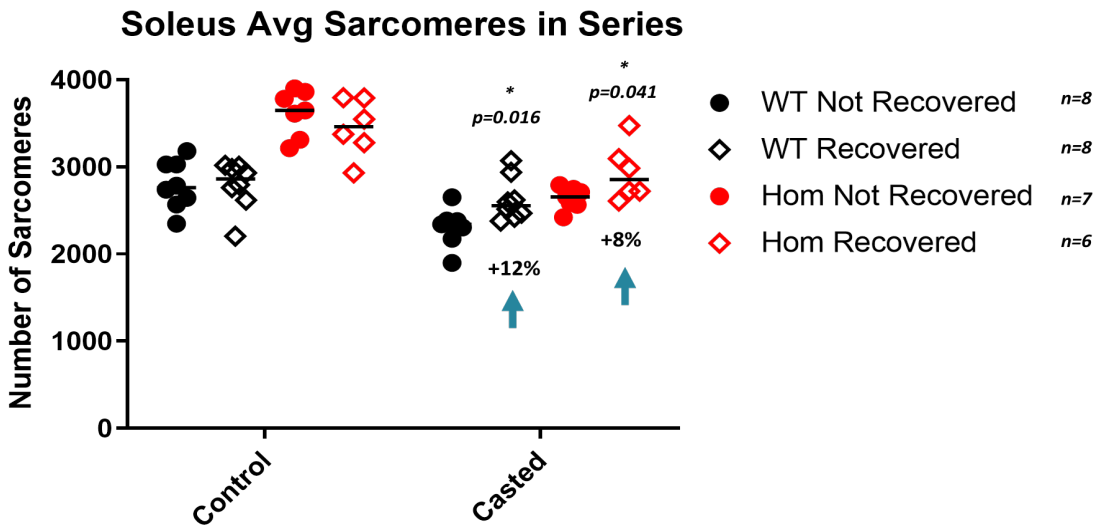

Figure 10 : Average sarcomeres in series of a soleus muscle from a 2 week Velcro cast immobilization of the hind limb (Non-recovered), and a 3.5-day recovery after removal of the velcro-cast (Recovered). WT Not Recovered tissues were represented by a black circle, WT Recovered tissues are represented by a black diamond outline. $Ttn^{\Delta 112-158}$ Not Recovered tissues were represented by a red circle. $Ttn^{\Delta 112-158}$ Recovered tissues were represented by a red diamond outline. WT casted soleus showed a 12% increase in a 3.5 day recovery from removal of cast. This increase is statistically significant (* p = 0.016). $Ttn^{\Delta 112-158}$ casted soleus showed an 8% increase in a 3.5 day recovery from removal of cast. This increase is statistically significant (* p = 0.041).

Discussion and Conclusions

5th Toe EDL Muscle Mechanics:

The 5th toe EDL muscle mechanic experiment illuminated an increase in weight in the stretched $Ttn^{\Delta 112-158}$ group (Fig 4). Pilot experiments were performed when the protocol was being optimized. Muscles were activated before and after the 90 min stretch-and-release protocol to verify viability of the muscle. These pilot studies showed that the muscles produce the same amount of force during activation before and after the experiment. This eliminates the possibility that $Ttn^{\Delta 112-158}$ muscles are being damaged or torn during the experiment allowing fluid buildup through the extracellular matrix (ECM), and thereby causing the increased weight in muscle. The exact cause behind the increased weight in stretched $Ttn^{\Delta 112-158}$ group has yet to be determined. One possibility is that mechanically-gated channels were opened, allowing physiological media to flow in at a greater rate in $Ttn^{\Delta 112-158}$ muscle as compared to WT [81] since $Ttn^{\Delta 112-158}$ muscle was experiencing more strain than WT. It is unlikely that the 90-min stretch-and-release protocol on the 5th toe EDL allows enough time for new protein synthesis to cause the weight difference. This is especially unlikely if the results from the hind limb experiment are taken into consideration (Fig 10). In the hind limb experiment, $Ttn^{\Delta 112-158}$ improved by 80 sarcomeres per day during the recovery period. Given these results, it can be predicted that 5 sarcomeres would be added to the muscle fibers during 90 min stretch protocol, which would not be enough mass to detectably contribute to the weight increase.

5th Toe EDL Muscle Proteomics

Synemin and SPEG were consistently upregulated in the $Ttn^{\Delta 112\text{-}158}$ mice relative to controls (Fig 9). Synemin (desmuslin) is an intermediate filament in the cytoskeleton that manages mechanical stress and maintains the structural integrity of a cell [82, 83]. It is localized at the Z-disk and binds to desmisn, α-dystrobrevin, α-actinin, and the extra cellular matrix (ECM) as a mechanical linker in transmitting force throughout the tissue. In simple terms, synemin links the costamere and the sarcomere in skeletal muscle.

Figure 7 depicts many differential phosphorylation sites on titin in the Z-disk region. And although synemin may not bind directly to titin, titin does insert in the Z-disk, perhaps causing changes to the proteins associated, and thereby enhancing synemin activity. Synemin also plays a role in PI3K-Akt and signaling pathways by participating in the PKA phosphoinositide 3-kinase [84]. In a study where synemin-deficient mice (Synm2/2) were generated; these mice displayed normal development and fertility and showed a mild degeneration and regeneration phenotype in the muscle fibers and mild different in the sarcolemma membrane [85]. Overall Synm2/2 mice muscles showed no difference in muscle mass and fiber type compared to control mice under normal physiological conditions [85]. However, in the absence of synemin, behavior of muscle satellite cells was affected, membrane integrity was reduced, and muscle fiber degeneration was seen [55]. With the constant repeated stretch of the 5th toe EDL, it is possible that the ECM is destabilized and triggers the PI3K-Akt signaling pathways, resulting in the production sarcomeric protein. Once longitudinal hypertrophy occurs in response to constant stretch perhaps the membrane proteins restabilize, and thereby turning off hypertrophy pathways.

Striated muscle-specific serine/threonine-protein kinase (SPEG) is required for myocyte cytoskeletal development of striated heart and skeletal muscle.[86] SPEG interacts with the protein obscurin, although its exact function is currently unclear. Obscurin proteins interact near the titin-kinase (TK) region [86]. SPEG proteins were upregulated and their interactions with obscurin could account for the elevated modifications in the TK region of the titin domain (Fig 7). Mutations in SPEG and obscurin resulting in heart disease such as hypertrophic cardiomyopathies, dilated cardiomyopathies, and left ventricular non-compaction cardiomyopathy have been studied in great detail [87]. Although mutations in these proteins in mice are lethal, making it difficult to study, especially on skeletal muscle, a conditional SPEG-knockout mouse model was developed to identify the mechanisms of skeletal muscle dysfunction due to SPEG deficiency [88]. While there was difference in body mass, size of muscle fibers, force generated in muscle and some structural issues, there was no difference in the total number of sarcomeres between normal muscle tissue and SPEG deficient muscle. SPEG does not appear to be a main contender in the contribution of longitudinal hypertrophy, but its interactions with obscurin and the TK region make it an intriguing protein to consider and could potentially determine TK catalytic activity.

Hind Limb Cast

After the cast was removed sarcomere absorption was measured in the soleus muscle. $Ttn^{\Delta 112\text{-}158}$ muscle (-70 sarcomeres per day) seem to have a rate of decrease 2x quicker than WT muscle (-36 sarcomere per day). I expected that the recovery, the increase of sarcomeres in series would have the same or similar trend as the decrease of sarcomeres between$Ttn^{\Delta 112\text{-}158}$ muscle and WT muscle. Also, $Ttn^{\Delta 112\text{-}158}$ mice would experience a greater strain that WT during the 3.5-day recovery, activating protein synthesis and adding sarcomeres in series at a greater rate than WT mice. However, based on the results from Figure 10, it seems that the recovered

$Ttn^{\Delta 112\text{-}158}$ casted muscle(+80 sarcomeres per day) did not have a higher rate of adding sarcomeres in series than recovered WT casted muscle (+104 sarcomeres per day). There was no statistical significance between the genotypes of mice. This supports the idea that the addition of sarcomeres in series is a rate limiting step and $Ttn^{\Delta 112\text{-}158}$ mice adapt at the same pace as WT for longer periods of time. A second time point would be needed to test this hypothesis. The recovery time of 3.5-days is not enough time for the casted legs to return to the sarcomeres in series to baseline conditions, however, it is enough time for the activation of longitudinal growth pathways.

Conclusion

In conclusion we have utilized a mutant mouse model, $Ttn^{\Delta 112\text{-}158}$, that has a stiffer titin molecule and has increased sarcomeres in series in skeletal muscle to probe longitudinal growth pathways. We have developed *ex vivo* and *in vivo* methods to test the hypothesis that mechanically coupled vectors of titin regulate longitudinal hypertrophy in skeletal muscle, and, as a result, an increase in titin-based stiffness will promote longitudinal hypertrophy. Proteins SPEG and synemin has been identified as consistently being upregulated in $Ttn^{\Delta 112\text{-}158}$ stretched muscle compared to controls. These proteins identify the Z-disk region and the M-Band region being highly active in activity during muscle stretch. The PI3-AKT pathway was identified as being involved in longitudinal hypertrophy, and an assay for follow up studies on probing this pathway has been developed

Future Directions

5th Toe EDL Muscle Mechanics and Proteomics

The 5th toe EDL muscle mechanics experimental groups have an n=2 value, even though each n-value is composed of a group of mice. It is possible to increase the n-value to n=4, either by continuing the number of experiments or combining the sexes into one group. The experiment included female and male groups. Although there are sex differences in the protein analysis (Fig 5), both male and female $Ttn^{\Delta 112\text{-}158}$ mice experienced longitudinal hypertrophy at equal rate increases [27]. Therefore, the pathway to longitudinal hypertrophy is most likely the same between the sexes. It would be logical to combine the proteomic results from both sexes into the experimental groups in order to compare solely treatment vs control.

Muscle Proteomics: Titin Kinase Activity

There are many phosphorylated proteins in the titin kinase/M-band region of titin (Fig 7), which is an area of great interest. There is debate in the scientific community on whether the titin kinase domain is a catalytic site or an inactive pseudo-kinase [54, 89]. Titin kinase has a dual-autoinhibition: an adenosine triphosphate (ATP) binding site that is blocked by a tail and a tyrosine base autoinhibition. It is theorized that external forces such as mechanical stretch removes the autoinhibitory tail by unfolding the TK domain, and thereby exposing the ATP-binding site to cause phosphorylation of tyrosine, which triggers a cascade of biochemical signals, ultimately leading to gene transcription [54]. The other argument is that the titin kinase has a non-detectable catalytic output, and instead, the TK has more involvement in muscle scaffolding than kinase activity [89]. The cellular pathway of the TK is poorly understood and controversial, the main issue is that TK activity has never been observed *in vivo*, only *in vitro*. Further probing this region using our mouse model could illuminate the activity and pathways that are triggered by titin kinase.

Longitudinal Hypertrophy Pathway Targetability

Probing the PI3-AKT pathway is essential to better understand the molecular mechanisms of

longitudinal hypertrophy. There have been many inhibitors developed for other disease that target certain areas of the PI3-AKT pathway especially in cancers. GSK3β inhibitors have been studied in diseases such as Alzheimer's [90], diabetes [91] and various cancers [92]. GSK3β is a protein that is elevated in our mutant mouse model undergoing stretch. One possibility to test this part of the pathway could be to add GSK3β inhibitors to the cell media and repeat the stretch mechanics experiment to determine if it blocks or alters the effects of the $Ttn^{\Delta 112-158}$mutant.

Recently synemin has been found to be a part of the PI3K-Akt signaling pathway [84]. Using synemin deficient mice could also help us probe another area of the PI3K-Akt pathway, or using inhibitors on synemin deficient mice in different parts of the pathway could be targeted for testing.

Hind Limb Cast:

The results from the hind limb cast showed that there seems to be no difference in rate of the addition of sarcomeres in series between $Ttn^{\Delta 112-158}$ and WT mice (Fig 10). This could be because the addition of sarcomeres is a rate limiting step, and that $Ttn^{\Delta 112-158}$ mice produce sarcomeres for more time than WT. This hypothesis could be tested by repeating the experiment and having a longer recovery time, such as 5 - 7 days, to track the addition of sarcomeres in series and see how long it takes for WT and $Ttn^{\Delta 112-158}$ mice to reach baseline numbers of sarcomeres in series in their casted leg.

Proteomic analysis on the casted muscle versus control muscle also needs to be completed. Ideally through the same MS process as the 5th Toe EDL. Proteins and pathways need to be identified that contribute to the addition of sarcomeres in series. This will prove challenging for many reasons. First, the soleus muscle has undergone significant atrophy and protein turnover as longitudinal growth is beginning to occur. This will add a level to complexity when doing protein and pathway analysis. Second, the soleus muscle may be experiencing activation of longitudinal growth pathways at the same time as cross-sectional growth, making it difficult to identify protein and pathways involved solely in longitudinal hypertrophy. During recovery, mice will be moving around normally causing contracting in the muscles and an increase in load will lead to cross-sectional growth. This problem could be solved by repeating the study and denervation of the lower limb after the cast is removed, potentially mimicking passive stretch during recovery.

Even though the soleus muscle is composed primarily of slow twitch muscles and the EDL is composed of fast twitch muscles, the proteins and pathways involved in longitudinal growth may not be different between muscle types. Both muscle types undergo similar levels of longitudinal hypertrophy [27] and therefore could experience regulation through the same growth pathways. This idea can be tested in future studies.

Appendix

Supplementary Data Mass Spectrometry Analysis

A study was performed to determine the least amount necessary for reliable results for phospho-proteomics (Table A). Table A indicated different samples based on tissue weight and the number of phospho-proteins in each sample. The largest increase in the number of phospo-proteins was from 16mg (513) of tissue to 24 mg (637) of tissue with a 43% increase. From 24 mg (637) to 32 mg (667) was a 4% increase, and a 6% increase from 32mg (667) to 40mg (680) (Table A).

Another strategy used on this test was to analyze the top ten phosphorylated genes and determined the difference between tissue amounts (Table B and Fig A). In Figure A, a parallel coordinate plot showed a massive increase in the total spectrum count between the tissue amount of 16mg to 24mg, and then a plateau between 24mg, 32, mg and 40 mg. This experiment helped determine that 30mg of fresh tissue would be enough to give reliable results on for proteomics study on the 5th toe EDL mechanics experiment

Phospho-Enrichment Results

mg tissue	# Spectra	# Proteins	# IDs	% IDs	# Phospho-proteins	# Phospho IDs	% Phospho IDs
16	225816	581	10576	4.7	513	6920	3.1
24	230164	696	14705	6.4	637	9906	4.3
32	232720	726	14915	6.4	667	10354	4.4
40	237109	777	17988	7.6	680	11017	4.6

Table A: Pilot phospho-enrichment test. Values of different peptides and peptide ID's from mass spectretry test on varying amounts mg of tissues.

Table B) ***Top Ten Genes with a Phospho Spectrum Count***

Total Spectrum Count with Phospho Filter								
		Sample amount		Sample amount		Sample amount		Sample amou
		16mg		24mg		32mg		40mg
Gene #	Gene Name		Gene Name		Gene Name		Gene NAme	
1	Ttn	1135	Ttn	1681	Ttn	1720	Ttn	1835
2	Myh4	373	Myh4	517	Myh4	548	Myh4	505
3	Myh1	295	Myh1	419	Myh1	446	Myh1	414
4	Myh8	186	Myh8	282	Myh8	292	Myh8	281
5	Srl	152	Naca	180	Acta1	232	Srl	231
6	Speg	128	Srl	179	Srl	205	Acta1	219
7	Naca	126	Acta1	178	Actc1	198	Naca	214
8	Acta1	124	Speg	160	Naca	186	Jph2	186
9	Obscn	108	Ckm	154	Actb	181	Actb	186
10	Jph2	108	Actg1	152	Jph2	175	Speg	170

Table B:) Table of Top Ten genes: the gene names, the sample amount with the corresponing phospho spectrum count.

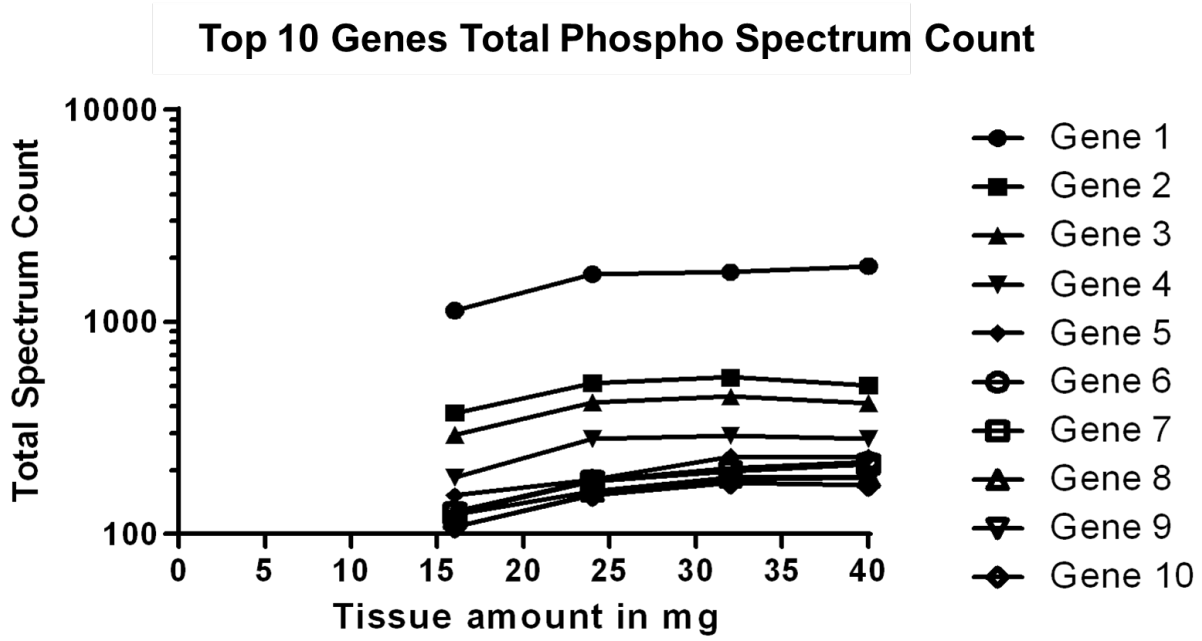

Figure A) Parallel coordinate plot of top ten genes from Table B and their total spectrum count (y-axis vs the tissue amount (x-axis)

References:

1. Dave, H.D., M. Shook, and M. Varacallo, *Anatomy, Skeletal Muscle*, in *StatPearls*. 2021: Treasure Island (FL).
2. Lindberg, M.R., . Lamps Laura W, *Diagnostic Pathology: Normal Histology (Second Edition)*

2018, Elsevier. p. 76-81.
3. Ehler, E. and M. Gautel, *The sarcomere and sarcomerogenesis.* Adv Exp Med Biol, 2008. **642**: p. 1-14.
4. Fluck, M. and H. Hoppeler, *Molecular basis of skeletal muscle plasticity--from gene to form and function.* Rev Physiol Biochem Pharmacol, 2003. **146**: p. 159-216.
5. Henderson, C.A., et al., *Overview of the Muscle Cytoskeleton.* Compr Physiol, 2017. **7**(3): p. 891-944.
6. Linke, W.A. and J.M. Fernandez, *Cardiac titin: molecular basis of elasticity and cellular contribution to elastic and viscous stiffness components in myocardium.* J Muscle Res Cell Motil, 2002. **23**(5-6): p. 483-97.
7. Srikakulam, R. and D.A. Winkelmann, *Chaperone-mediated folding and assembly of myosin in striated muscle.* J Cell Sci, 2004. **117**(Pt 4): p. 641-52.
8. Sanger, F., S. Nicklen, and A.R. Coulson, *DNA sequencing with chain-terminating inhibitors.* Proc Natl Acad Sci U S A, 1977. **74**(12): p. 5463-7.
9. Sanger, J.W., et al., *Myofibrillogenesis in skeletal muscle cells.* Clin Orthop Relat Res, 2002(403 Suppl): p. S153-62.
10. Sorimachi, H., et al., *Tissue-specific expression and alpha-actinin binding properties of the Z-disc titin: implications for the nature of vertebrate Z-discs.* J Mol Biol, 1997. **270**(5): p. 688-95.
11. Turnacioglu, K.K., et al., *Partial characterization of zeugmatin indicates that it is part of the Z-band region of titin.* Cell Motil Cytoskeleton, 1996. **34**(2): p. 108-21.
12. Young, P., et al., *Molecular structure of the sarcomeric Z-disk: two types of titin interactions lead to an asymmetrical sorting of alpha-actinin.* EMBO J, 1998. **17**(6): p. 1614-24.
13. Van der Loop FTL, V.d.V.P., Fürst DO et al, *Integration of titin into the sarcomeres of cultured differentiating human skeletal muscle cells.* Eur J Cell Biol, 1996. **69**: p. 301-307.
14. Yang, Y.G., T. Obinata, and Y. Shimada, *Developmental relationship of myosin binding proteins (myomesin, connectin and C-protein) to myosin in chicken somites as studied by immunofluorescence microscopy.* Cell Struct Funct, 2000. **25**(3): p. 177-85.
15. Komiyama, M., K. Maruyama, and Y. Shimada, *Assembly of connectin (titin) in relation to myosin and alpha-actinin in cultured cardiac myocytes.* J Muscle Res Cell Motil, 1990. **11**(5): p. 419-28.
16. Witt, C.C., et al., *Nebulin regulates thin filament length, contractility, and Z-disk structure in vivo.* EMBO J, 2006. **25**(16): p. 3843-55.
17. Weitzer, G., et al., *Cytoskeletal control of myogenesis: a desmin null mutation blocks the myogenic pathway during embryonic stem cell differentiation.* Dev Biol, 1995. **172**(2): p. 422-39.
18. Li, Z., et al., *Cardiovascular lesions and skeletal myopathy in mice lacking desmin.* Dev Biol, 1996. **175**(2): p. 362-6.
19. Milner, D.J., et al., *Disruption of muscle architecture and myocardial degeneration in mice lacking desmin.* J Cell Biol, 1996. **134**(5): p. 1255-70.
20. van der Ven, P.F., et al., *A functional knock-out of titin results in defective myofibril assembly.* J Cell Sci, 2000. **113 (Pt 8)**: p. 1405-14.
21. Xu, X., et al., *Cardiomyopathy in zebrafish due to mutation in an alternatively spliced exon of titin.* Nat Genet, 2002. **30**(2): p. 205-9.

22. Gotthardt, M., et al., *Conditional expression of mutant M-line titins results in cardiomyopathy with altered sarcomere structure.* J Biol Chem, 2003. **278**(8): p. 6059-65.
23. Bang, M.L., et al., *The complete gene sequence of titin, expression of an unusual approximately 700-kDa titin isoform, and its interaction with obscurin identify a novel Z-line to I-band linking system.* Circ Res, 2001. **89**(11): p. 1065-72.
24. Furst, D.O., et al., *The organization of titin filaments in the half-sarcomere revealed by monoclonal antibodies in immunoelectron microscopy: a map of ten nonrepetitive epitopes starting at the Z line extends close to the M line.* J Cell Biol, 1988. **106**(5): p. 1563-72.
25. Grater, F., et al., *Mechanically induced titin kinase activation studied by force-probe molecular dynamics simulations.* Biophys J, 2005. **88**(2): p. 790-804.
26. Granzier, H.L. and S. Labeit, *The Giant Protein Titin: A Major Player in Myocardial Mechanics, Signaling, and Disease.* Circulation Research, 2004. **94**(3): p. 284-295.
27. Brynnel, A., et al., *Downsizing the molecular spring of the giant protein titin reveals that skeletal muscle titin determines passive stiffness and drives longitudinal hypertrophy.* Elife, 2018. **7**.
28. Horowits, R. and R.J. Podolsky, *The positional stability of thick filaments in activated skeletal muscle depends on sarcomere length: evidence for the role of titin filaments.* J Cell Biol, 1987. **105**(5): p. 2217-23.
29. Roy, A., et al., *Measurement of passive ankle stiffness in subjects with chronic hemiparesis using a novel ankle robot.* J Neurophysiol, 2011. **105**(5): p. 2132-49.
30. Linke, W.A. and M.C. Leake, *Multiple sources of passive stress relaxation in muscle fibres.* Phys Med Biol, 2004. **49**(16): p. 3613-27.
31. Trombitas, K., et al., *Molecular basis of passive stress relaxation in human soleus fibers: assessment of the role of immunoglobulin-like domain unfolding.* Biophys J, 2003. **85**(5): p. 3142-53.
32. Hornberger, T.A., et al., *Aging does not alter the mechanosensitivity of the p38, p70S6k, and JNK2 signaling pathways in skeletal muscle.* J Appl Physiol (1985), 2005. **98**(4): p. 1562-6.
33. Krzysztofik, M., et al., *Maximizing Muscle Hypertrophy: A Systematic Review of Advanced Resistance Training Techniques and Methods.* Int J Environ Res Public Health, 2019. **16**(24).
34. Schoenfeld, B.J., *The mechanisms of muscle hypertrophy and their application to resistance training.* J Strength Cond Res, 2010. **24**(10): p. 2857-72.
35. Goktepe, S., et al., *A multiscale model for eccentric and concentric cardiac growth through sarcomerogenesis.* J Theor Biol, 2010. **265**(3): p. 433-42.
36. Kerckhoffs, R.C., J. Omens, and A.D. McCulloch, *A single strain-based growth law predicts concentric and eccentric cardiac growth during pressure and volume overload.* Mech Res Commun, 2012. **42**: p. 40-50.
37. Schuelke, M., et al., *Myostatin mutation associated with gross muscle hypertrophy in a child.* N Engl J Med, 2004. **350**(26): p. 2682-8.
38. Adams, G.R., *Insulin-like growth factor in muscle growth and its potential abuse by athletes.* Br J Sports Med, 2000. **34**(6): p. 412-3.
39. Sakuma, K. and A. Yamaguchi, *The functional role of calcineurin in hypertrophy, regeneration, and disorders of skeletal muscle.* J Biomed Biotechnol, 2010. **2010**: p. 721219.
40. Vlachou, M., et al., *Does tendon lengthening surgery affect muscle tone in children with cerebral palsy?* Acta Orthop Belg, 2009. **75**(6): p. 808-14.
41. Ottenheijm, C.A., et al., *Titin-based mechanosensing and signaling: role in diaphragm atrophy during unloading?* Am J Physiol Lung Cell Mol Physiol, 2011. **300**(2): p. L161-6.
42. Kruger, M. and S. Kotter, *Titin, a Central Mediator for Hypertrophic Signaling, Exercise-Induced Mechanosignaling and Skeletal Muscle Remodeling.* Front Physiol, 2016. **7**: p. 76.

43. van der Pijl, R.J., et al., *Deleting Titin's C-Terminal PEVK Exons Increases Passive Stiffness, Alters Splicing, and Induces Cross-Sectional and Longitudinal Hypertrophy in Skeletal Muscle.* Front Physiol, 2020. **11**: p. 494.
44. van der Pijl, R., et al., *Titin-based mechanosensing modulates muscle hypertrophy.* J Cachexia Sarcopenia Muscle, 2018. **9**(5): p. 947-961.
45. Knoll, R., et al., *The cardiac mechanical stretch sensor machinery involves a Z disc complex that is defective in a subset of human dilated cardiomyopathy.* Cell, 2002. **111**(7): p. 943-55.
46. Olson, E.N. and R.S. Williams, *Calcineurin signaling and muscle remodeling.* Cell, 2000. **101**(7): p. 689-92.
47. Miller, M.K., et al., *The muscle ankyrin repeat proteins: CARP, ankrd2/Arpp and DARP as a family of titin filament-based stress response molecules.* J Mol Biol, 2003. **333**(5): p. 951-64.
48. Barash, I.A., et al., *Structural and regulatory roles of muscle ankyrin repeat protein family in skeletal muscle.* Am J Physiol Cell Physiol, 2007. **293**(1): p. C218-27.
49. Lange, S., et al., *MLP and CARP are linked to chronic PKCalpha signalling in dilated cardiomyopathy.* Nat Commun, 2016. **7**: p. 12120.
50. Witt, S.H., et al., *MURF-1 and MURF-2 target a specific subset of myofibrillar proteins redundantly: towards understanding MURF-dependent muscle ubiquitination.* J Mol Biol, 2005. **350**(4): p. 713-22.
51. Moriscot, A.S., et al., *MuRF1 is a muscle fiber-type II associated factor and together with MuRF2 regulates type-II fiber trophicity and maintenance.* J Struct Biol, 2010. **170**(2): p. 344-53.
52. Hirner, S., et al., *MuRF1-dependent regulation of systemic carbohydrate metabolism as revealed from transgenic mouse studies.* J Mol Biol, 2008. **379**(4): p. 666-77.
53. Lange, S., et al., *The kinase domain of titin controls muscle gene expression and protein turnover.* Science, 2005. **308**(5728): p. 1599-603.
54. Puchner, E.M., et al., *Mechanoenzymatics of titin kinase.* Proc Natl Acad Sci U S A, 2008. **105**(36): p. 13385-90.
55. Friden, J. and R.L. Lieber, *Spastic muscle cells are shorter and stiffer than normal cells.* Muscle Nerve, 2003. **27**(2): p. 157-64.
56. Ottenheijm, C.A. and H. Granzier, *Role of titin in skeletal muscle function and disease.* Adv Exp Med Biol, 2010. **682**: p. 105-22.
57. Lieber, S.D.a.R.L., *Muscle Changes at the Cellular-Fiber Level in Cerebral Palsy*, in *Cerebral Palsy*, B.S. Miller F., Lennon N., O'Neil M. (eds), Editor. 2018, Springer, Cham.
58. Ottenheijm, C.A., et al., *Titin and diaphragm dysfunction in chronic obstructive pulmonary disease.* Am J Respir Crit Care Med, 2006. **173**(5): p. 527-34.
59. Lieber, R.L., et al., *Skeletal muscle mechanics, energetics and plasticity Daniel P Ferris.* Journal of NeuroEngineering and Rehabilitation, 2017. **14**(1): p. 1-16.
60. Institute of Laboratory Animal Resources (U.S.). Committee on Revision of the Guide for Laboratory Animals Facilities and Care., Institute of Laboratory Animal Resources (U.S.). Committee on the Guide for Laboratory Animal Facilities and Care., and Animal Care Panel (U.S.). Animal Facilities Standards Committee., *Guide for laboratory animal facilities and care*, in *Publication / Public Health Service*. U.S. Public Health Service : For sale by the Supt. of Docs.: Bethesda, Md.
61. Lieber, R.L. and J. Friden, *Functional and clinical significance of skeletal muscle architecture.* Muscle Nerve, 2000. **23**(11): p. 1647-66.
62. Chleboun, G.S., T.J. Patel, and R.L. Lieber, *Skeletal muscle architecture and fiber-type distribution with the multiple bellies of the mouse extensor digitorum longus muscle.* Acta Anat (Basel), 1997. **159**(2-3): p. 147-55.

63. Lieber, R.L. and S.R. Ward, *Skeletal muscle design to meet functional demands.* Philos Trans R Soc Lond B Biol Sci, 2011. **366**(1570): p. 1466-76.
64. Dayanidhi, S., et al., *Does a Reduced Number of Muscle Stem Cells Impair the Addition of Sarcomeres and Recovery from a Skeletal Muscle Contracture? A Transgenic Mouse Model.* Clin Orthop Relat Res, 2020. **478**(4): p. 886-899.
65. Hidalgo, C., C. Saripalli, and H.L. Granzier, *Effect of exercise training on post-translational and post-transcriptional regulation of titin stiffness in striated muscle of wild type and IG KO mice.* Arch Biochem Biophys, 2014. **552-553**: p. 100-7.
66. Team, R.C., *R: A language and environment for statistical computing.* R Foundation for Statistical Computing, 2021.
67. Carlson M, M.B., *UniProt.ws: R Interface to UniProt Web Services. .* R package version 2.34.0., 2021.
68. Hadley, W., *stringr: Simple, Consistent Wrappers for Common String Operations. .* R package version 1.4.0., 2019.
69. Kolde, R., *Pretty Heatmaps. .* R package version 1.0.12., 2019.
70. Xiaofei Zhang, A.H.S., Gabrielle B.A. van Tilburg, Huib Ovaa, Wolfgang Huber and Michiel Vermeulen, *Proteome-wide identification of ubiquitin interactions using UbIA-MS* Nature Protocols, 2018.
71. Ritchie, M.E., et al., *limma powers differential expression analyses for RNA-sequencing and microarray studies.* Nucleic Acids Res, 2015. **43**(7): p. e47.
72. Kevin Blighe, S.R.a.M.L., *EnhancedVolcano: Publication-ready volcano plots with enhanced colouring and labeling.* R package version 1.12.0. , 2021
73. Sievert, C., *Interactive Web-Based Data Visualization with R, plotly, and shiny.* . Chapman and Hall/CRC Florida, 2020.
74. Calin Voichita, S.A.a.S.D., *ROntoTools: R Onto-Tools suite. .* R package version 2.22.0., 2021
75. Luo, W. and C. Brouwer, *Pathview: an R/Bioconductor package for pathway-based data integration and visualization.* Bioinformatics, 2013. **29**(14): p. 1830-1.
76. King, D., D. Yeomanson, and H.E. Bryant, *PI3King the lock: targeting the PI3K/Akt/mTOR pathway as a novel therapeutic strategy in neuroblastoma.* J Pediatr Hematol Oncol, 2015. **37**(4): p. 245-51.
77. Craig, E.A., J.S. Weissman, and A.L. Horwich, *Heat shock proteins and molecular chaperones: mediators of protein conformation and turnover in the cell.* Cell, 1994. **78**(3): p. 365-72.
78. Lindquist, S., *The heat-shock response.* Annu Rev Biochem, 1986. **55**: p. 1151-91.
79. (NCBI)[Internet], N.C.f.B.I., *MAPK1 mitogen-activated protein kinase 1 [Homo sapiens* N.L.o.M. (US, Editor., National Center for Biotechnology Information: Bethesda (MD).
80. Williams, P.E. and G. Goldspink, *The effect of immobilization on the longitudinal growth of striated muscle fibres.* J Anat, 1973. **116**(Pt 1): p. 45-55.
81. Stiber, J.A., M. Seth, and P.B. Rosenberg, *Mechanosensitive channels in striated muscle and the cardiovascular system: not quite a stretch anymore.* J Cardiovasc Pharmacol, 2009. **54**(2): p. 116-22.
82. Garcia-Pelagio, K.P., et al., *Absence of synemin in mice causes structural and functional abnormalities in heart.* J Mol Cell Cardiol, 2018. **114**: p. 354-363.
83. Garcia-Pelagio, K.P., et al., *Myopathic changes in murine skeletal muscle lacking synemin.* Am J Physiol Cell Physiol, 2015. **308**(6): p. C448-62.
84. Russell, M.A., *Synemin Redefined: Multiple Binding Partners Results in Multifunctionality.* Front Cell Dev Biol, 2020. **8**: p. 159.
85. Li, Z., et al., *Synemin acts as a regulator of signalling molecules during skeletal muscle hypertrophy.* J Cell Sci, 2014. **127**(Pt 21): p. 4589-601.

86. Fleming, J.R., et al., *Exploring Obscurin and SPEG Kinase Biology.* J Clin Med, 2021. **10**(5).
87. Marston, S., et al., *OBSCN Mutations Associated with Dilated Cardiomyopathy and Haploinsufficiency.* PLoS One, 2015. **10**(9): p. e0138568.
88. Huntoon, V., et al., *SPEG-deficient skeletal muscles exhibit abnormal triad and defective calcium handling.* Hum Mol Genet, 2018. **27**(9): p. 1608-1617.
89. Bogomolovas, J., et al., *Titin kinase is an inactive pseudokinase scaffold that supports MuRF1 recruitment to the sarcomeric M-line.* Open Biol, 2014. **4**(5): p. 140041.
90. Griebel, G., et al., *The selective GSK3 inhibitor, SAR502250, displays neuroprotective activity and attenuates behavioral impairments in models of neuropsychiatric symptoms of Alzheimer's disease in rodents.* Sci Rep, 2019. **9**(1): p. 18045.
91. Ali, A., K.P. Hoeflich, and J.R. Woodgett, *Glycogen synthase kinase-3: properties, functions, and regulation.* Chem Rev, 2001. **101**(8): p. 2527-40.
92. Sayas, C.L., et al., *GSK-3 is activated by the tyrosine kinase Pyk2 during LPA1-mediated neurite retraction.* Mol Biol Cell, 2006. **17**(4): p. 1834-44.